

https://dspace.org/

In silico analysis of the melamine structural analogues interaction with calciumsensing receptor A potential for nephrotoxicity

Mandisi Sithole; Gary Gabriels; Thankhoe Rants'o

https://hdl.handle.net/10539/44753
SCOPUS

Downloaded from a DSpace repository. https://dspace.org/

Computational Toxicology 32 (2024) 100333

Contents lists available at ScienceDirect

Computational Toxicology

journal homepage: www.sciencedirect.com/journal/computational-toxicology

Full Length Article

In silico analysis of the melamine structural analogues interaction with calcium-sensing receptor: A potential for nephrotoxicity

Mandisi Sithole [a], Gary Gabriels [a], Thankhoe A. Rants'o [b,c,*]

[a] *Pharmacology Division, Department of Pharmacy and Pharmacology, Faculty of Health Sciences, University of the Witwatersrand, Johannesburg, Gauteng, 2193, South Africa*
[b] *Department of Pharmacology and Toxicology, University of Utah, Salt Lake City, Utah, 84112, USA*
[c] *Huntsman Cancer Institute, Department of Medicine, University of Utah, Salt Lake City, Utah, 84112, USA*

ARTICLE INFO

Keywords:
Cyanuric acid
G-protein coupled receptors
Melamine cyanurate
Molecular modelling
Nephrotoxicity

ABSTRACT

In recent years, melamine, and its structural analogues, as adulterants in various food products including protein supplements, have been widely studied for their nephrotoxic effects. Previous research has presented evidence that certain small molecules can alter the calcium-sensing receptor (CaSR) function, contributing to nephrotoxicity. Melamine, for example, has been observed in *in vitro* settings to interact with the allosteric binding site of CaSR, resulting in uncontrolled CaSR activation. This activation results in the production of reactive oxygen species, which eventually causes kidney cell apoptosis and/or necrosis. The present research used the *in silico* molecular modelling to evaluate the CaSR binding profiles of four common adulterants in protein supplements: melamine, cyanuric acid, uric acid, and melamine cyanurate. Using Schrödinger's Maestro docking software (version 13.2.128), the docking studies coupled a noncovalent extra precision mode with the molecular mechanics-generalized born surface area (MM-GBSA) simulation for enhanced binding affinity prediction accuracy. This study identified that cyanuric acid, uric acid, and melamine cyanurate have greater CaSR binding affinities than melamine. Interestingly, melamine cyanurate had the highest binding potential to CaSR. Previous animal studies have reported high concentrations of melamine cyanurate complex in rat kidneys following melamine administration. These findings demonstrate a molecular explanation melamine cyanurate complex-induced nephrotoxicity. This research offers new insight regarding the probable mechanism through which melamine, its analogues, and complexes may cause nephrotoxicity.

1. Introduction

Melamine and its structural analogues, such as cyanuric acid, and melamine cyanurate, have been implicated as adulterants in a variety of protein-rich foods and supplements [1,2]. Proteins are highly nitrogenous compounds made of amino acid building blocks [3]. Due to the structural similarity to amino acids and these compounds along with their high nitrogen content (Fig. 1), are attractive as adulterants in protein supplements [1,4]. However, research has revealed that consuming these in copious quantities or at low doses over extended time periods can have a range of adverse effects, with nephrotoxicity being the most apparent and well-studied [5]. Nephrotoxicity refers to the damage or injury to the kidneys caused by exposure to certain drugs, toxins, or other substances which results in impaired kidney function or renal failure [6]. Various studies have demonstrated that endogenous uric acid interacts with melamine and its analogues, forming complexes that induce nephrotoxicity [7,8]. Although there is extensive evidence that these substances induce kidney damage through the formation of kidney stones, renal injury, and nephrotoxicity, the underlying mechanisms of these health consequences remain largely unknown [9].

Significant insights into the underlying processes by which melamine and related compounds cause renal damage have been gained from both *in vitro* and *in vivo* studies. In one study, the effects of melamine and cyanuric acid on the kidney health of children, aged 4 to 8 years were examined by measuring the levels of these compounds in the children's urine samples and investigating the associated markers of renal impairment [10]. Despite equivalent exposure levels, the data indicated that female participants exhibited higher levels of kidney damage biomarkers than the male participants. This correlates with the gender differences in the global burden of kidney disease where women are

* Corresponding author.
E-mail address: Thankhoe.Rantso@pharm.utah.edu (T.A. Rants'o).

https://doi.org/10.1016/j.comtox.2024.100333
Received 30 January 2024; Received in revised form 10 October 2024; Accepted 11 October 2024
Available online 15 October 2024
2468-1113/© 2024 The Author(s). Published by Elsevier B.V. This is an open access article under the CC BY-NC license (http://creativecommons.org/licenses/by-nc/4.0/).

affected more than men. For example, in 2019, it was reported that 417 million women suffered from kidney disease in comparison to 336 million men [11]. Furthermore, the combination of melamine and cyanuric acid was more nephrotoxic with elevation of multiple renal damage markers [10]. Another study investigated the effects of co-exposure to melamine and oxalate on human renal proximal tubular cells to [12]. This co-exposure resulted in increased oxidative stress, mitochondrial dysfunction, tubular cell apoptosis, and fibrosis. This suggested that melamine, even at concentrations considered safe when administered alone, can induce significant renal damage when combined with other nephrotoxicants such as oxalates [12]. These studies elucidated the mechanisms by which melamine can cause kidney damage, particularly when combined with other environmental toxicants, and underscored the importance of considering co-exposure risks and sex-specific responses when evaluating melamine toxicity.

Crystallization and urinary supersaturation are the common mechanisms of kidney stone formation [13]. Research has revealed a correlation between high concentrations of calcium within renal epithelial cells and the presence of melamine in the serum [9,13]. It has also been demonstrated that melamine exacerbates calcium oxalate crystal formation, a common kidney stone which in turn leads to renal failure [9,12,13]. Interestingly, in the presence of gut microbiota, melamine has also been shown to undergo a conversion to cyanuric acid, a derivative that rapidly forms a complex with melamine [14]. The melamine cyanurate crystals in kidneys have been shown to be more important in melamine-induced nephrotoxicity [14]. The influx of calcium ions intracellularly is believed to play a role in the regulation of apoptosis [4,15,16]. The high intracellular calcium influx is attributed to the disruption of the endoplasmic reticulum (ER) caused by an imbalance in calcium homeostasis. This interference results in ER stress and subsequent release of calcium from calcium stores in the ER, ultimately leading to the downstream activation of apoptosis in renal epithelial cells [15,16].

Kidney retention of the crystals and their attachment to the renal epithelium is mainly dependent on their interaction with local receptors such as calcium-sensing receptors (CaSRs) [13]. CaSRs are G-protein coupled receptors that are responsible for regulating calcium homeostasis in the human body [17,18]. These receptors are localized in parathyroid glands and the kidneys (proximal tubule, distal tubule and collecting ducts) where they respectively play these important roles: (i) influence parathyroid hormone synthesis, a hormone that regulates calcium levels, and (ii) regulate calcium reabsorption from the kidneys [16,17,18].

Previous studies have suggested that the activation of CaSRs in the

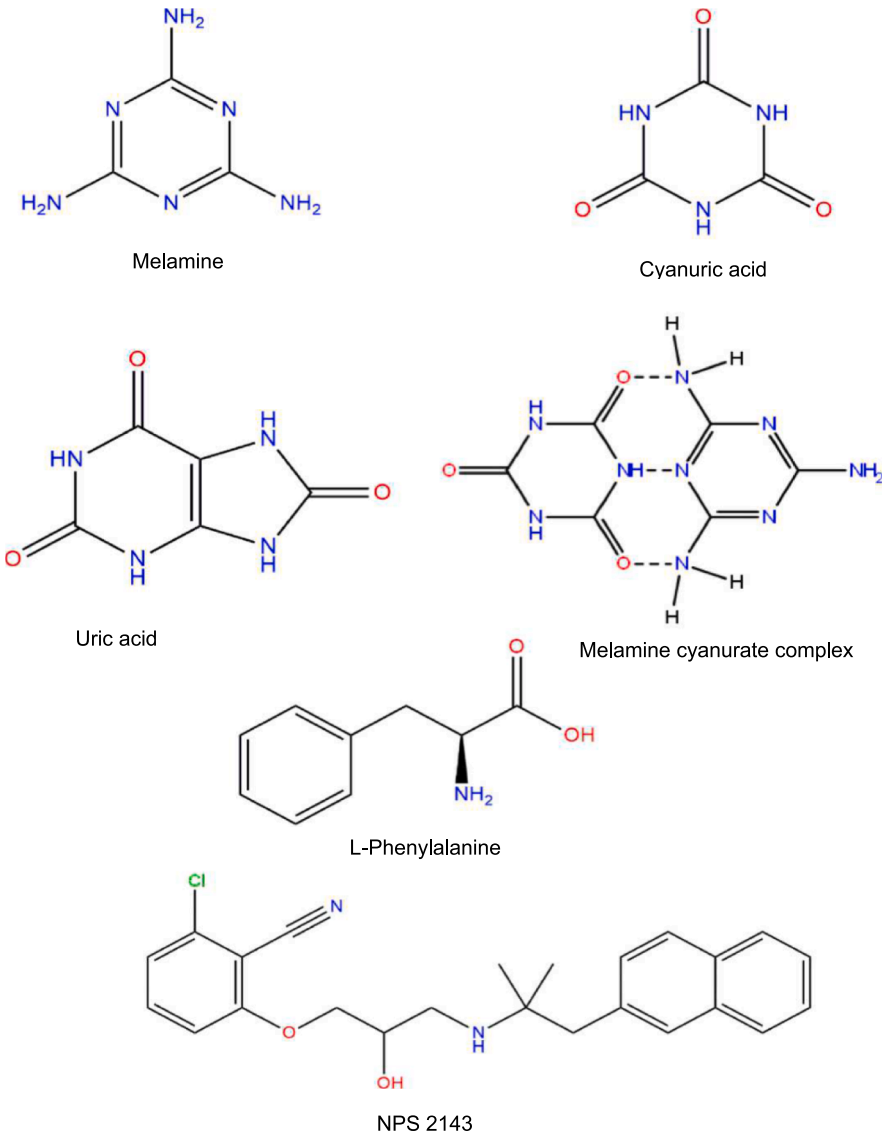


Fig. 1. Chemical structures of ligands used against CaSR.

kidneys may result in nephrotoxicity [4,18,19]. Gibbons *et al* demonstrated that the activation of CaSRs by an antibiotic gentamicin in the proximal convoluted tubules, resulted in caspase-mediated renal cell death [19]. Additionally, an *in vitro* cell culture study by Yiu *et al* found that melamine could allosterically activate CaSR in renal epithelial cells, resulting in increased calcium entry and increased production of reactive oxygen species and subsequent apoptosis [4]. Consequently, it is proposed that melamine activation of CaSR is the upstream mechanism that signals a sustained intracellular rise in calcium concentration, hence causing renal epithelial cell injury and apoptosis [4].

Over the past few decades, computational approaches have played an essential role in drug discovery by predicting and finding specific ligand binding sites within proteins [20,21]. The identification of these sites within a protein or receptor has benefited in the exploration of intermolecular interaction mechanisms and effectively explains disease pathophysiology, offering insight for drug discovery, design, and development [21]. The advantage of computational techniques, over highly precise but time-consuming and expensive biological research, is that ligand binding site predictions may be made using sequence and structural data, rather than annotating the biological function of protein binding residues [21,22].

The computational approach known as molecular mechanics-generalized born surface area (MM-GBSA) simulation is used in molecular modelling studies to determine the binding free energy between a protein and a ligand [23,24]. MM-GBSA has various computational benefits and applications, making it an effective method for predicting the binding affinity of ligands to proteins [23]. MM-GBSA has been shown to allow a flexible, predictive, and accurate approach in assessing ligand interactions with the receptors providing high correlation to the experimental data [23,24,25]. Traditional free energy calculation methods, such as free energy perturbation calculations and molecular dynamics simulations, are slower and more tedious than MM-GBSA calculations [24,26]. Therefore, MM-GBSA is less computationally costly than these other approaches making it a viable and efficient alternative for high-throughput virtual screening of large compound libraries [25,26,27]. The MM-GBSA approach is versatile and adaptable, as it can be applied to a wide range of systems, including protein–protein interactions, protein–ligand interactions, and protein-DNA interactions [25,28]. In addition, MM-GBSA accounts for solvation effects by simulating the interaction of docked ligands with a solvent through solvent models, explicit solvation algorithms, and advanced docking software [23,29]. This molecular mechanics-based approach can also be employed to investigate protein conformational changes and protein–ligand binding kinetics [24,27]. Also, it can provide accurate insight into the contributions of various interactions, including van der Waals interactions, electrostatic interactions, and solvation effects [28,30].

In summary, MM-GBSA provides a versatile, accurate, and computationally efficient approach for estimating the free energy of ligand binding to proteins in docking studies. It is a useful and efficient tool for high-throughput virtual screening of large compound libraries, and MM-GBSA versatility and flexibility make it applicable to a wide range of systems [23,25].

There has been limited research into the interactions of melamine, cyanuric acid, uric acid, and melamine cyanurate with biological proteins using computational approaches. The current study employed a classical noncovalent docking mode coupled to the MM-GBSA simulation to explore the protein binding profiles of melamine and its derivatives with a select CaSR associated with the induction of nephrotoxic effects. This study provides novel insights into how individual adulterants and their complexes may induce nephrotoxicity through CaSR activation through this novel docking approach.

2. Materials and methods

2.1. Target protein preparation

Schrödinger Release 2022–2 docking suite, Maestro version 13.2.128 (Schrödinger, LLC, New York) was used for the docking studies. While it has been suggested that CaSR agonists such as calcium stabilize the active state of the receptor, it has also been shown that calcium and L-amino acids to bind on the allosteric site of the inactive form of the receptor to induce its activation and downstream effects [18,31]. As a result, this study selected CaSR protein (PDB ID: 7E6T) from the Protein Data Bank (PDB). Selection of the 7E6T crystal structure was based on its active form, presence of important components in the binding site such as Ca^{2+} and PO_4^{3-} which are reported to play a key role in CaSR stabilization as well as retention of the active form [16]. The crystal structure had a resolution of 3 Å and was in a ligand-bound state with L-Tryptophan (L-Trp). For the docking study, the protein crystal structure was prepared using a protein preparation wizard program. The first step was to pre-process the imported 7E6T followed by removal of water molecules located more than 3 Å from the binding site and could make less than 3H-bonds with a receptor or ligand. Removing water molecules that do not play a role in ligand-binding has been shown to improve the accuracy of binding affinity prediction [21]. Non-protein hetero groups were also eliminated, and any missing hydrogens, side chains, or loops were completed. Utilizing the computational tool in Maestro suite, PROPKA, the protonation and ionization states for the 7E6T protein was optimized for docking at pH 7.0 [21]. The final stage was protein minimization using the OPLS4e force field to resolve all molecular overlaps and strains [32].

2.2. Receptor grid generation

Based on the homodimer nature of the human CaSRs, the 7E6T protein was prepared with two identical chains (A and B) [16]. Both chains have similar ligand-binding sites with residues that are similar to those described in the literature [18,31]. Therefore, the chains were split with only chain A used for grid generation and further docking studies. Given the ligand-bound state of 7E6T, the same ligand was utilized to define the allosteric site during grid generation using the OPLS4e force field [32].

2.3. Ligand preparation

The PubChem database was used to obtain the chemical structures of ligands including the allosteric inducers and inhibitors of CaSR, L-phenylalanine (L-Phe) and NPS 2143, respectively, which were used as reference compounds [31]. The investigative ligands melamine, cyanuric acid, uric acid, and melamine cyanurate complex, along with the reference molecules are illustrated in Fig. 1. The Maestro 2D Sketcher was used to draw the ligand structures [24]. Following this, the ligands were prepared using LigPrep, and possible ionization and tautomeric states were generated using the pKa prediction program, Epik at pH 7.0 (± 2.0). Moreover, each ligand was allowed to generate up to 32 stereoisomeric forms [24]. Similarly, OPLS4e force field was used to minimize the ligands [32].

2.4. Noncovalent docking of ligands against CaSR

The ligands utilized in this study were initially docked to 7E6T using the extra precision (XP) mode, which has been shown to intense rigor and high accuracy [24]. These ligands were allowed to be flexible in XP mode to allow for the most precise docking [32]. Following this procedure, the binding conformations and glide scores of all docked compounds were recorded. In order to validate the docking method, reference compounds were docked first, and their binding profiles compared to the literature.

2.5. MM-GBSA based simulation of ligands against CaSR

The evaluation of ligand binding affinities to CaSR was conducted using Prime MM-GBSA-based simulations [22]. The noncovalent complexes previously docked in the XP platform were retrieved, and the solvation model VSGB and OPLS4e force field were employed in this re-docking phase. The ligand distance was increased to 5 Å to permit flexibility of the target protein [22]. The re-docking was executed, and the obtained binding affinities were subsequently compared.

3. Results

3.1. Noncovalent docking of ligands against CaSR

CaSR is a transmembrane receptor that exists as a homodimer (Fig. 2), with two identical chains [4,18,33]. Both chains' allosteric binding sites are on the extracellular side, and the amino acid residues inside the binding sites include, among others, Ser^{147}, Ser^{170}, Thr^{145}, Ala^{168}, Tyr^{218}, and Glu^{297} [18,33]. The standard CaSR modulators L-Phe and NPS 2143 each formed four residue interactions at the binding site (Fig. 3). On the other hand, all the investigated adulterants including melamine, cyanuric acid, uric acid, and melamine cyanurate, formed interactions with at least two allosteric site residues after noncovalent docking (Fig. 4). The ligands in this study were found to interact with these residues through H-bonds, salt bridges, and π-π stacking interactions. In both the ligands and the allosteric site resides, H-bonds primarily occurred between the carboxyl oxygen and hydrogen of an amide group (Fig. 3 and Fig. 4).

L-Phe made four H-bonds from three catalytic residues (Fig. 3A). This includes one H-bond with Ser^{170} and another with Ala^{168}, as well as two H-bonds with Ser^{147} (Fig. 3A). Glu^{297} produced a salt bridge between its carboxyl group oxygen and an amide group hydrogen on L-Phe (Fig. 3A). Four catalytic residues in NPS 2143 formed H-bonds. Ser^{147} had two H-bonds with NPS 2143, whereas Ala^{168}, Thr^{145}, and Gly^{148} all had one H-bond with NPS 2143 (Fig. 3B).

Similar residues that interacted with the reference compounds were also important in the binding of test adulterants. In particular, melamine established two H-bonds (Fig. 4A), one with Ser^{170} and the other with Glu^{297}. Cyanuric acid also formed two H-bonds with serine residues Ser^{170} and Ser^{147}, respectively (Fig. 4B). On the other hand, uric acid had three H-bonds, two with Ser^{147} and one with Ala^{168} (Fig. 4C). Interestingly, melamine-cyanurate had one H-bond with Ser^{147} and two with Glu^{297} (Fig. 4D).

Melamine cyanurate additionally produced a salt bridge between the hydrogen on the amide group, and the oxygen of a carboxyl group from Glu^{297} (Fig. 4D). Moreover, noncovalent docking of the protein supplement adulterants produced poses which interacted mainly with two of the binding site residues (Table 2).

Table 1 shows the glide-dock scores for the ligands varied from −6.74 to −3.25 kcal/mol. Melamine had the lowest glide-dock score among the adulterants, at −3.25 kcal/mol, whereas melamine-cyanurate had the highest, at −6.74 kcal/mol (Table 1). The CaSR negative modulator, NPS 2143 had a higher glide-dock at −6.37 kcal/mol compared to −3.75 kcal/mol for L-Phe (Table 1). Noncovalent glide-dock scores did not demonstrate a significant difference between adulterants and CaSR modulators in general (Table 1).

3.2. Simulation of ligands against CaSR using MM-GBSA

The interactions between the ligands and CaSR following Prime MM-GBSA re-docking differed for several of the ligands from the noncovalent docking interactions (Table 2). The poses generated by the MM-GBSA simulations were closer to the allosteric site and the ligands interacted mostly with the binding site amino acid residues (Table 2). Furthermore,

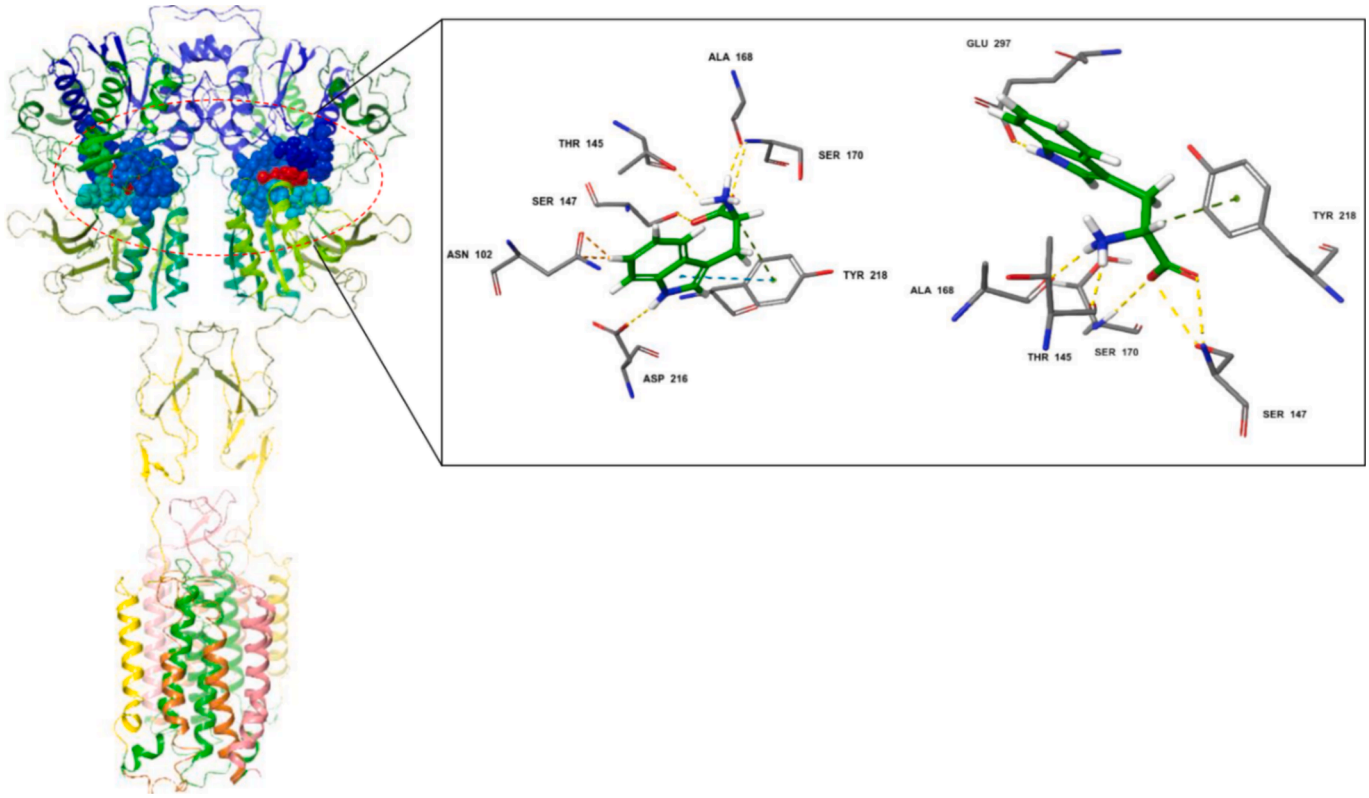


Fig. 2. The homodimer structure of CaSR with the generated docking of L-Trp in both chains. (A) L-Trp bound to active sites of CaSR in chains A and B. (B) CaSR binding sites with interacting amino residues (grey) and L-Trp (green). The binding energy for L-Trp in chain A was determined to be −30.50 kcal/mol and −28.83 kcal/mol in chain B. (For interpretation of the references to colour in this figure legend, the reader is referred to the web version of this article.)

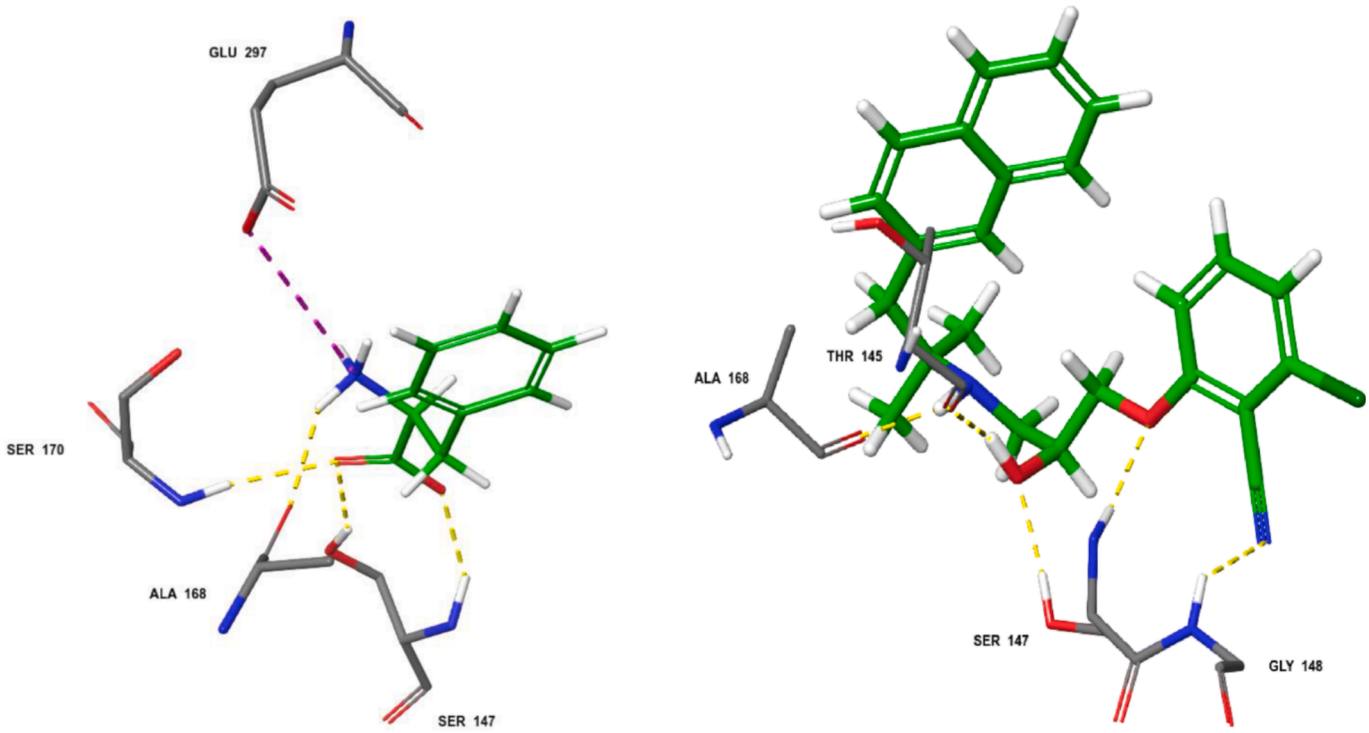


Fig. 3. Noncovalent docking of positive and negative allosteric modulators in the CaSR allosteric site with interacting residues. (A) L-Phenylalanine and (B) NPS 2143.

all ligands in the MM-GBSA simulation were ranked according to the lowest to the highest binding energies, with a significant difference in binding energy scores between the ligands (Table 1).

With the exception of an extra H-bond from Ser^{147} (Fig. 5A), the positive allosteric modulator of CaSR, L-Phe, maintained the same pose and binding residue interactions in MM-GBSA (Table 2). However, among the ligands investigated in this study, its binding energy of −27.15 kcal/mol was the second lowest (Table 1). Similarly, NPS 2143 MM-GBSA docking resulted in the identical catalytic residue contacts as noncovalent docking, apart from an extra interaction with Ser^{147}, which formed three H-bonds (Fig. 5B). NPS 2143, on the other hand, had the greatest binding energy of the ligands studied, with −66.68 kcal/mol (Table 1).

Melamine established one H-bond with each of the three residues, Ser^{147}, Ser^{170}, and Ala^{168} (Fig. 6A). Melamine had a binding energy of −25.8 kcal/mol, which was lower than the other ligands and in correlation with the initial XP docking (Table 1). In addition to Ser^{147} and Ser^{170} interactions that were also obtained in XP docking, cyanuric acid interacted with Thr^{145} through a single aromatic H-bond and Tyr^{218} via a π-π stacking between the aromatic rings (Fig. 6B). Cyanuric acid had a binding energy of −29.7 kcal/mol, which was slightly higher than L-Phe (Table 1). The two H-bonds with Ser^{147} were sustained by uric acid, but instead of Ala^{168}, the configuration in MM-GBSA caused an H-bond contact with the Ser^{170} (Fig. 6C). In comparison to noncovalent docking, melamine cyanurate formed three H-bond interactions with Ser^{147} (Fig. 6D). In addition, the melamine cyanurate MM-GBSA docking mode produced catalytic interactions with Ser^{170} and Thr^{145} via a single H-bond each, as well as Tyr^{218} via a π-π stacking between the benzene rings (Fig. 6D). Still, melamine cyanurate had the highest binding energy among the adulterants, at −43.58 kcal/mol.

4. Discussion

In this study the interactions of the ligands used, namely melamine, cyanuric acid, uric acid, melamine cyanurate, L-Phe, and NPS 2143 occurred within the allosteric site of the CaSR, thereby validating the binding site as previously reported in other studies [18]. The type of interactions between the ligands and the residues observed were via H-bonds, salt bridges, and π-π stacking interactions. Most interactions between the adulterants and binding site residues were H-bonds, except for melamine cyanurate, which formed a salt bridge with Glu^{297} (Fig. 4). H-bonds between binding site amino acids and proteins are critical for receptor recognition, specificity, and subsequent activation [34,35]. In this respect, all the ligands utilised in this study had carboxyl and amide groups, which were critical in the formation of H-bonds via intermolecular interactions between a hydrogen atom and an electronegative atom, such as the oxygen atom from a carboxyl group or the nitrogen atom in an amide group [36,37]. In addition, the noncovalent mode observed in this study, produced poses which were distant from most binding site amino acid residues which is consistent with the study of Rants'o *et al* [24].

The Prime MM-GBSA re-docking of the ligands of interest, on the contrary, resulted in poses that had improved amino acid residue interactions within the binding pocket (Table 2). This supports previous findings that MM-GBSA scoring, and pose-generating functions yield more accurate results compared to the noncovalent mode [24,38]. After MM-GBSA re-docking, the catalytic Tyr^{218} established π-π stacking interactions with both cyanuric acid (Fig. 6B) and melamine cyanurate (Fig. 6D). The π-π stacking interactions increase stability, which aids in the retention of the ligand within the binding pocket [39,40]. Several studies have previously demonstrated the importance of Tyr within a catalytic site [18,19,24]. Tyr has been shown to have the ability to form H-bonds with non-aromatic ligands or establish aromatic interactions with aromatic ligands in order to enhance ligand stability inside the binding pocket [18,19,24]. Furthermore, MM-GBSA produced poses for the adulterants that were closer to the CaSR binding pocket. For example, while cyanuric acid had just two residue contacts in the noncovalent docking mode, cyanuric acid had two additional residue interactions in MM-GBSA docking, with Tyr^{218} and Thr^{145} (Table 2). A comparable improvement was observed with melamine with two contacts from Ala^{168} and Ser^{147}, and with melamine cyanurate with three additional interactions from Ser^{147}, Tyr^{218}, and Thr^{145}. These findings

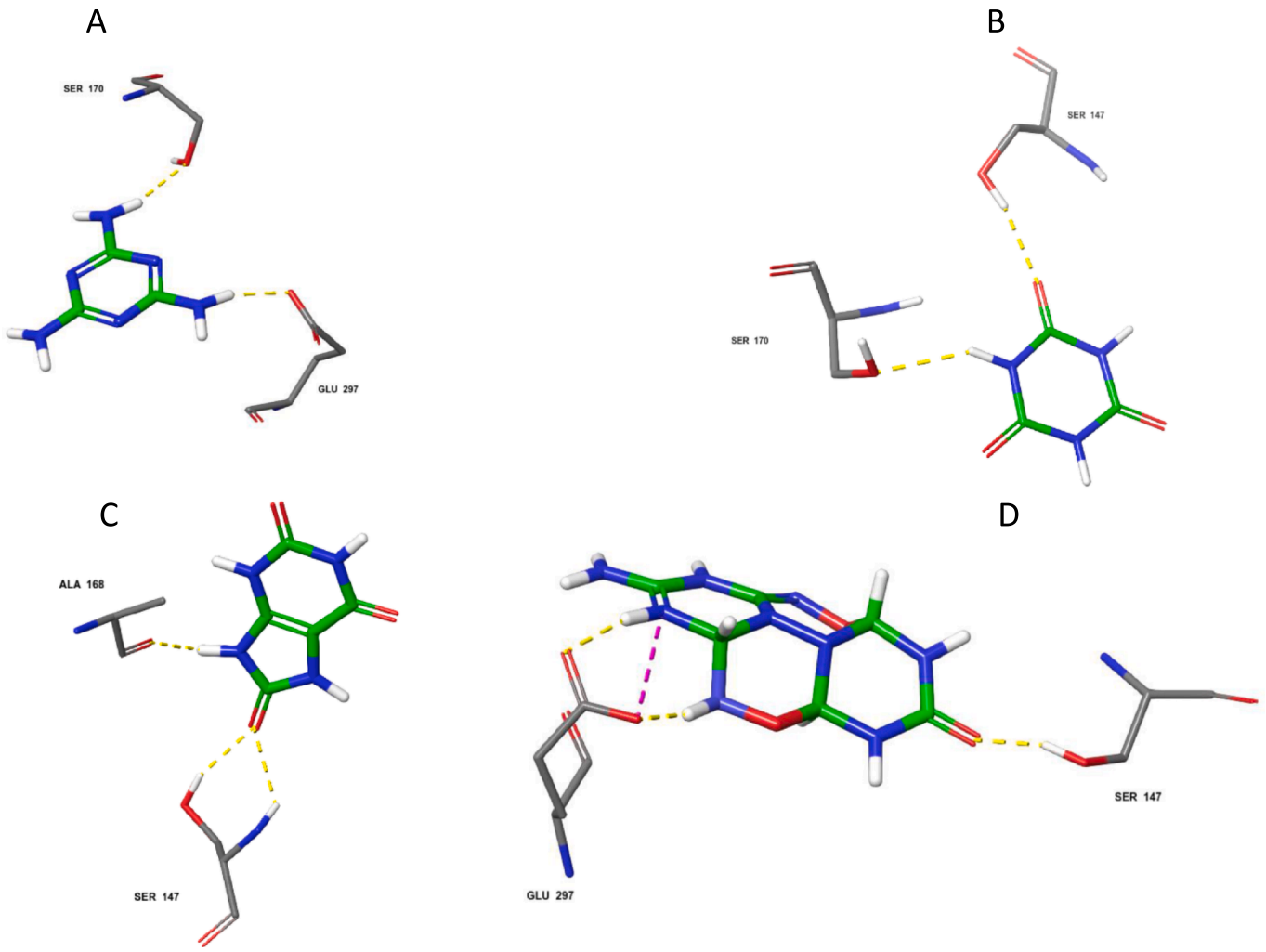


Fig. 4. Noncovalent docking of ligands in the CaSR allosteric site with interacting residues. (A) Melamine, (B) Cyanuric acid, (C) Uric acid and (D) Melamine cyanurate complex.

Table 1
Glide docking and binding energy scores of ligands bonded to CaSR.

Compound	Docking score XP (kcal/mol)	Glide-dock XP (kcal/mol)	MM-GBSA (kcal/mol)
Melamine	−3.25	−3.25	−25.80
L-Phe	−3.75	−3.75	−27.15
Cyanuric acid	−2.94	−3.55	−29.70
Uric acid	−2.02	−4.18	−36.01
Melamine cyanurate	−6.18	−6.74	−43.58
NPS 2143	−3.95	−6.37	−66.68

Table 2
Amino acid residues interactions in the binding of select ligands against CaSR in noncovalent docking and MM-GBSA re-docking.

Compound	Glide-dock XP	MM-GBSA
Melamine	Ser^{170}, Glu^{297}	Ser^{170}, Ser^{147}, Ala^{168}
Cyanuric acid	Ser^{170}, Ser^{147}	Ser^{170}, Ser^{147}, Tyr^{218}, Thr^{145}
Uric acid	Ser^{170}, Ala^{168}	Ser^{170}, Ser^{147}
Melamine cyanurate	Ser^{147}, Glu^{297}	Ser^{170}, Ser^{147}, Tyr^{218}, Thr^{145}
L-Phe	Ser^{170}, Ser^{147}, Ala^{168}, Glu^{297}	Ser^{170}, Ser^{147}, Ala^{168}, Glu^{297}
NPS 2143	Ser^{147}, Ala^{168}, Thr^{145}, Gly^{148}	Ser^{147}, Ala^{168}, Thr^{145}, Gly^{148}

confirm previous evidence that supplementing noncovalent docking with MM-GBSA helps in identifying some of the key amino acid residues for accurate ligand binding and pose generation [24].

The MM-GBSA assessment also revealed higher binding affinity scores when compared to noncovalent docking scores (Table 1). MM-GBSA analysis showed that NPS 2143, a known CaSR inhibitor, had the highest binding energy of all the compounds investigated, at −66.68 kcal/mol (Table 1). This finding is consistent with previous studies by Yiu *et al* and Chen *et al*, which suggest that NPS 2143 is a potent inhibitor [4,41]. NPS 2143, a selective CaSR inhibitor, has been demonstrated to successfully prevent lipopolysaccharide-induced acute lung injury in an *in vitro* study by Lee *et al* [42]. This suggests that NPS 2143 could potentially be used as a therapeutic agent for countering the adverse effects of melamine and its related substances. Melamine cyanurate exhibited the highest binding energy of the adulterants studied. Furthermore, melamine-cyanurate demonstrated a higher binding affinity of −43.58 kcal/mol than the allosteric activator, L-Phe (Table 1). The increased binding affinity of the melamine-cyanurate complex suggests that it may be more potent than melamine, cyanuric acid, or uric acid, individually. This finding is similar to previous *in vitro* studies, which showed that creating the melamine cyanurate complex leads to a more stable complex with a higher risk of kidney damage [43,44]. As a result, this supports the literature that MM-GBSA can distinguish between closely similar ligand structures and offer correct poses and affinity ranking [24,45,46].

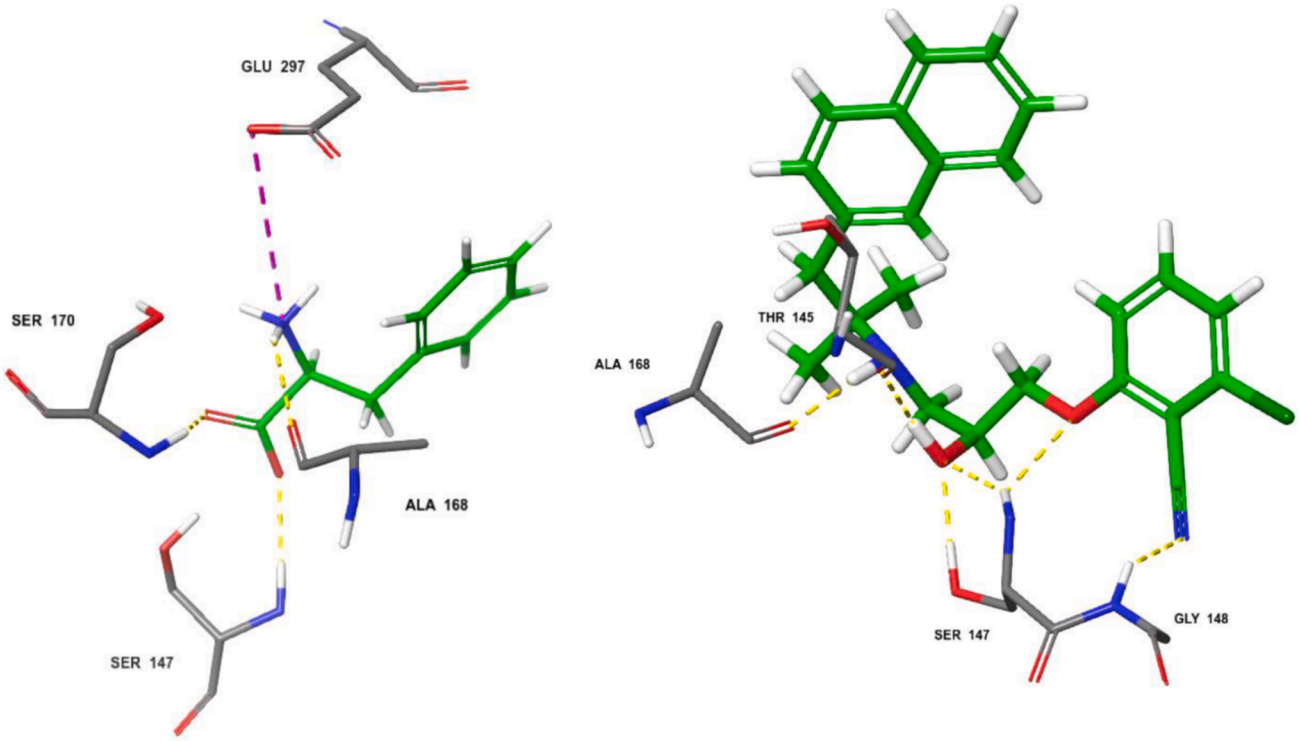


Fig. 5. MM-GBSA re-docking of positive and negative allosteric modulators in the CaSR active site with interacting residues. (A) L-Phenylalanine and (B) NPS 2143.

When the intermolecular interactions of melamine and the catalytic residues were compared to those of cyanuric acid, it was illustrated that cyanuric acid had more residue interactions than melamine (Fig. 6). This is since, while melamine has three amide moieties (–NH2) linked to the triazine ring, cyanuric acid has three carboxyl groups (–COOH) attached. Cyanuric acid is more electronegative than melamine because oxygen has a greater electronegativity than nitrogen [47]. This difference in electronegativity induces an increase in H-bond attraction, and the formation of π-π stacking interactions, as demonstrated with cyanuric acid (Fig. 6B) [24,47]. Furthermore, the cyanuric acid moiety participates in more hydrogen bonding and π-π stacking interactions than the melamine moiety in the melamine cyanurate structure (Fig. 6D). Melamine cyanurate has a more intricate structure, with numerous aromatic rings in the molecule, which increases the structures electronegativity [47]. Similarly, the imidazole moiety of uric acid, contributes to the formation of H-bonds more than the pyrimidine moiety (Fig. 6C).

The findings of this study provide the rationale for the adulterants' binding affinity and order, which is as follows: melamine cyanurate > uric acid > cyanuric acid > melamine. This correlates with previous research that suggest that the combination of melamine, cyanuric acid, and/or uric acid may be more nephrotoxic than the individual compounds alone [4]. A recent study revealed that a combination of melamine and cyanuric acid generated severe neurotoxic consequences, including cell death, disturbed energy generation, and decreased synaptic function, as opposed to the individual administration of these adulterants [48]. It further showed that melamine and cyanuric acid increased the levels of reactive oxygen species (ROS) that in turn promoted the apoptosis [48]. Indeed, the ROS scavenger *N*-acetylcysteine prevented the apoptosis induction from melamine and cyanuric acid [48]. Another study by Day *et al* which demonstrated how melamine and cyanuric acid synergistically intensify the nephrotoxic effects of these substances, supports this [10]. Additionally, Yiu *et al*'s *in vitro* investigation revealed that melamine could exert nephrotoxic effects by binding to CaSR [4]. These studies corroborate the findings of the current study, which demonstrated that while individual adulterants have an affinity for CaSR, co-exposure to these substances may result in more severe renal effects. Our finding that melamine has lower binding affinity to CaSR than when combined with cyanuric acid suggests that the co-exposure to melamine and its derivatives may result in more pronounced nephrotoxic effects. This is particularly important given that the gut microbiota often converts melamine to cyanuric acid resulting in the presence of both melamine and cyanuric acid in the systemic circulation [14]. The combined presence of melamine and cyanuric acid could result in the production of insoluble crystals in the kidney, which can eventually lead to renal failure [1,14,49,50]. Similarly, the combination of melamine and uric acid has been proven to induce kidney injury due to crystal formation and oxidative stress generation [4]. Hence it is critical to assess the potential harmful consequences of similar substances in combination rather than individually.

This study presents a novel approach to investigating the molecular docking of melamine, cyanuric acid, uric acid, and melamine cyanurate with CaSR using protein–ligand interactions. This research for the first time explored the interactions for these compounds in depth. The results demonstrate that the adulterants, namely melamine, cyanuric acid, uric acid, and melamine cyanurate, exhibit higher and comparable binding affinities for CaSR compared to its allosteric modulators, such as L-Trp (Fig. 2) and L-Phe (Table 1). Thus, based on the findings of this study, it can be deduced that melamine, cyanuric acid, uric acid, and melamine cyanurate, can allosterically activate the CaSR. Yiu *et al* previously demonstrated that melamine uncontrollably activates CaSR, resulting in a cascade of events that produce nephrotoxicity [4]. Based on this knowledge, the current study suggests cyanuric acid, uric acid, and melamine cyanurate behave similarly to melamine when analysed alone, as demonstrated by earlier research [4], potentially contributing to the cascade of events that lead to nephrotoxicity. Furthermore, the findings of this study support prior studies suggesting that melamine has a stronger nephrotoxic effect when combined with the other investigated adulterants in this study. The higher binding affinities identified for these compounds compared to melamine in this present investigation might explain the enhanced toxicity [4,44,47,49,51]. Therefore, this work, using a novel *in silico* approach, has shown the molecular basis by

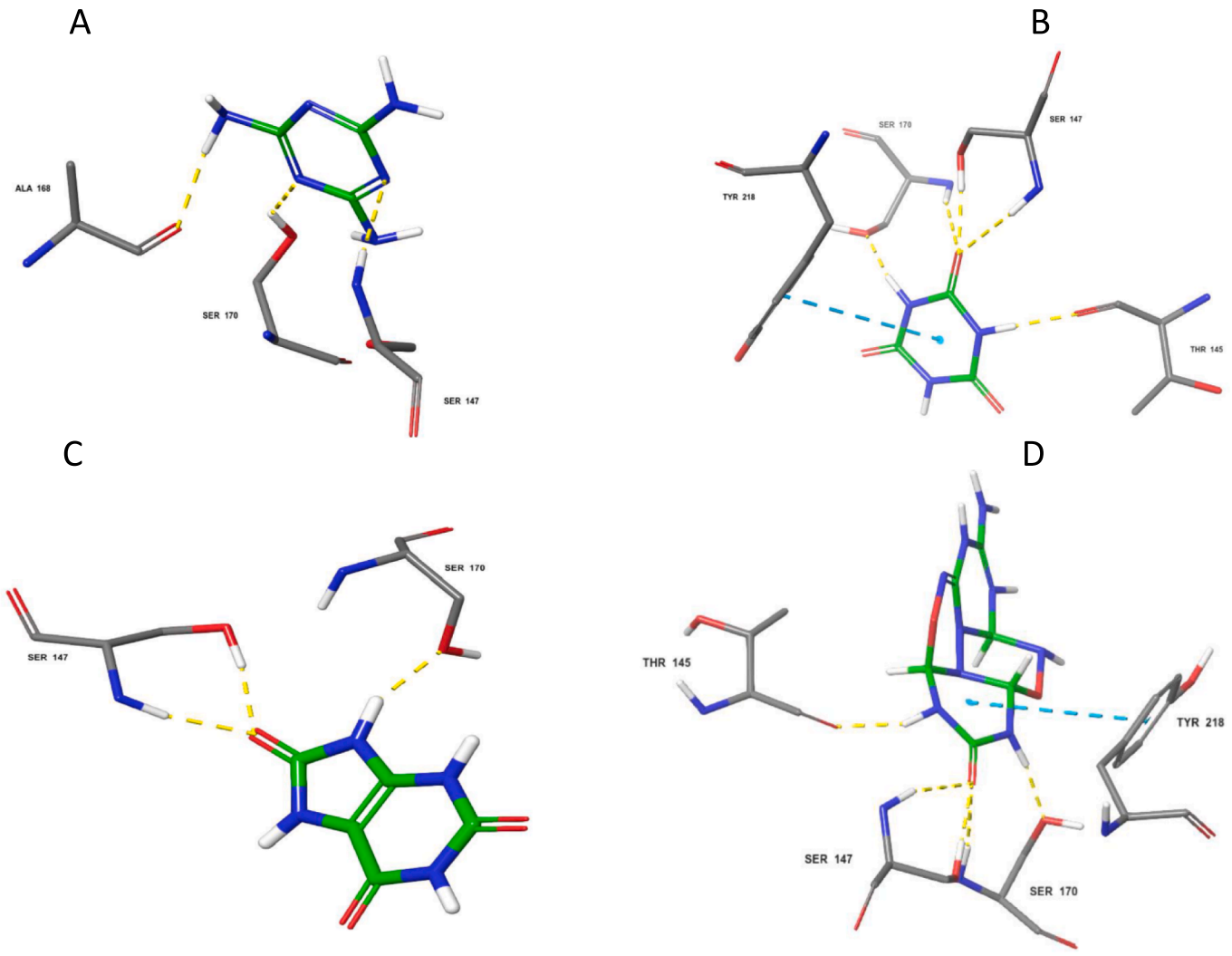


Fig. 6. MM-GBSA re-docking of ligands in the CaSR active site with interacting residues. (A) Melamine, (B) Cyanuric acid, (C) Uric acid and (D) Melamine cyanurate complex.

which melamine and its analogues can confer nephrotoxic effects. The use of *in silico* tools presents a viable approach for enhancing the efficacy of chemical risk assessments by identifying potential toxicological hazards and prioritizing compounds for subsequent *in vitro* and *in vivo* experiments, as exemplified by melamine and its analogues observed in the current study [52].

In summary, this research provides insights concerning the molecular docking of melamine, cyanuric acid, uric acid, and melamine cyanurate with CaSR. The findings indicate that these adulterants can allosterically activate CaSR, potentially causing nephrotoxicity. These findings add to what is previously known in the literature and expand the understanding of the mechanisms underlying the interactions between these adulterants and CaSR, highlighting the necessity of considering binding affinities when assessing toxicological impact. Future research ought to explore the precise mechanisms by which these ligands interact with CaSR, as well as strategies to mitigate their adverse effects. This work should include *in vitro* and *in vivo* animal studies that will assess the activation of CaSR by cyanuric acid, uric acid, and melamine cyanurate. This kind of investigation would verify the findings of the current study.

5. Conclusion

In this study, the binding affinities of melamine, cyanuric acid, uric acid, and melamine cyanurate, with CaSR using noncovalent docking and MM-GBSA modes were explored. Based on the MM-GBSA simulation, known to be highly accurate in affinity prediction, the interactions of the ligands with the catalytic residues were primarily H-bonds, with carboxyl and amide groups playing important roles in the generation of H-bonds and the recognition of the binding site via intermolecular interactions. While interactions such as aromatic H-bonds and π-π stacking provide more stability for the ligand-CaSR complex. Furthermore, the study showed that melamine cyanurate exhibited the highest binding affinity among the investigated compounds, while melamine displayed the lowest. The higher binding affinity of the melamine cyanurate complex indicates a stronger interaction with renal CaSR, leading to the formation of more stable complexes and potentially more harmful effects on the kidney epithelial cells. Thus, this study suggests that melamine cyanurate complex may be a more potent nephrotoxic agent than the other assessed protein supplement adulterants. The study provides new insights into the molecular mechanisms by which melamine and its analogues may induce nephrotoxic effects. The findings of this study may direct further studies in human toxicology into the possible protein supplement adulterants responsible for nephrotoxic effects. This study recommends further investigations of melamine cyanurate for nephrotoxic effects in *ex vivo* and *in vivo* models.

CRediT authorship contribution statement

Mandisi Sithole: Investigation, Formal analysis, data curation, Writing-original draft preparation. **Gary Gabriels:** Supervision, Project administration, Resources, Funding acquisition, Writing- reviewing and editing. **Thankhoe A. Rants'o:** Supervision, Conceptualization, Methodology, Software, Validation, Resources, Writing- reviewing and editing.

Declaration of competing interest

The authors declare that they have no known competing financial interests or personal relationships that could have appeared to influence the work reported in this paper.

Acknowledgements

The authors would like to thank Centre for High Performance Computing (CHPC)/Council for Scientific and Industrial Research (CSIR) for providing access to the molecular docking software, and research grant support from the South African Medical Research Council, and the South African National Research Foundation.

Data availability

Data will be made available on request.

References

[1] G. Gabriels, M. Lambert, P. Smith, D. Hiss, Melamine contamination in nutritional supplements – it is an alarm bell for the general consumer, athletes And 'weekend Warriors', Nutri. J. 14 (69) (2015) https://doi.org/10.1186/s12937-015-0055-7.
[2] E. García-Miguel, O.G. Meza-Márquez, G. Osorio-Revilla, D.I. Téllez-Medina, M. Jiménez-Martínez, D.M. Cornejo-Mazón, T.-V. Hernández-Martínez, Detection of cyanuric acid and melamine in infant formula powders by Mid-FTIR spectroscopy and multivariate analysis, J. Food Qual. (2018) 1–7, https://doi.org/10.1155/2018/7926768.
[3] S.K. Saha N.N. Pathak Proteins and Other Nitrogenous Substances of Nutritional Significance Fundamentals of Animal Nutrition 2021 Springer Singapore 10.1007/978-981-15-9125-9_7.
[4] A.J. Yiu, C.L. Ibeh, S.K. Roy, B.C. Bandyopadhyay, Melamine induces Ca2+-sensing receptor activation and elicits apoptosis in proximal tubular cells, Amer. J. Physio. Cell. Physio. 313 (1) (2017) 27–41, https://doi.org/10.1152/ajpcell.00225.2016.
[5] A.L. Bolden, J.R. Rochester, C.F. Kwiatkowski, Melamine beyond the kidney a ubiquitous endocrine disruptor and neurotoxicant? Tox. Letters. 280 (2017) 181–189, https://doi.org/10.1016/j.toxlet.2017.07.893.
[6] C. Liu, T. Hsieh, C. Wu, C. Lee, Y. Tsai, T. Huang, S. Wen, C. Lee, T. Chien, Y. Lee, S. Huang, C. Li, Y. Chou, W. Wu, M. Wu, Interrelationship of environmental melamine exposure, biomarkers of oxidative stress and early kidney injury, J. Haz. Mater. 396 (2020), https://doi.org/10.1016/j.jhazmat.2020.122726.
[7] N. Rai, D. Banerjee, R. Bhattacharyya, Urinary melamine: proposed parameter of melamine adulteration of food, Nutrition. 30 (4) (2014) 380–385, https://doi.org/10.1016/j.nut.2013.07.013.
[8] W.C. Li, C.F. Chow, Adverse child health impacts resulting from food adulterations in the Greater China Region, J. Sci. Food. Agri. 97 (2017), https://doi.org/10.1002/jsfa.8405.
[9] P. Thanasekaran, C. Liu, J. Cho, K. Lu, Melamine-promoted crystal growth of calcium oxalate monohydrate from calcium nitrate and oxalic acid, Inorg. Chem. Comm. 17 (2012) 84–87, https://doi.org/10.1016/j.inoche.2011.12.020.
[10] D.B. Day, M.M. Melough, J.T. Flynn, H. Zhu, K. Kannan, J. Ruzinski, I.H. de Boer, S. Sathyanarayana, Environmental exposure to melamine and its derivatives and kidney outcomes in children, Environ. Res. 252 (2024), https://doi.org/10.1016/j.envres.2024.118789.
[11] L.A. Tomlinson, C.M. Clase, Sex and the Incidence and Prevalence of Kidney Disease,Clinic.J.Amer.Soc.Nephro.,14(11) (2019),1557–1559, https://doi.org/10.2215/CJN.11030919.
[12] M.T. Wu, C.F. Wu, C.C. Liu, Y.C. Tsai, C.C. Chen, Y.H. Wang, T.J. Hsieh, Melamine and oxalate coexposure induces early kidney tubular injury through mitochondrial aberrations and oxidative stress, Ecotoxicol. Environ. Saf. 225 (2021), https://doi.org/10.1016/j.ecoenv.2021.112756.
[13] Z. Wang, Y. Zhang, J. Zhang, Q. Deng, H. Liang, Recent advances on the mechanisms of kidney stone formation (Review), Int. J. Mol. Med. 48 (2) (2021), https://doi.org/10.3892/ijmm.2021.4982.
[14] X. Zheng, A. Zhao, G. Xie, Y. Chi, L. Zhao, H. Li, C. Wang, Y. Bao, W. Jia, M. Luther, M. Su, J.K. Nicholson, W. Jia, Melamine-induced renal toxicity is mediated by the gut microbiota, Sci. Transl. Med. 13 (172) (2013), https://doi.org/10.1126/scitranslmed.3005114.
[15] B. Bánfi, F. Tirone, I. Durussel, J. Knisz, P. Moskwa, G.Z. Molnár, K.H. Krause, J. A. Cox, Mechanism of Ca activation of the NADPH oxidase 5 (NOX5), J. Biol. Chem. 279 (2004) 18583–18591, https://doi.org/10.1074/jbc.M310268200.
[16] C.T. Wu, T.I. Weng, L.P. Chen, C.K. Chiang, S.H. Liu, Involvement of caspase-12-dependent apoptotic pathway in ionic radiocontrast urografin-induced renal tubular cell injury, Toxicol. Appl. Pharmacol. 266 (2013) 167–175, https://doi.org/10.1016/j.taap.2012.10.012.
[17] T. Nakagawa, H. Zhu, N. Morishima, E. Li, J. Xu, B.A. Yankner, J. Yuan, Caspase-12 mediates endoplasmicreticulum-specific apoptosis and cytotoxicity by amyloid-beta, Nat. 403 (2000) 98–103, https://doi.org/10.1038/47513.
[18] Y. Geng, L. Mosyak, I. Kurinov, H.Zuo, E. Sturchler, T.C. Cheng, P. Subramanyam, A.P. Brown, S.C. Brennan, H. Chang, M. Bush, Y. Chen, T.X. Nguyen, B.Cao, D.D. Chang, M. Quick, A.D. Conigrave, H.M. Colecraft, P. McDonald, Q.R. Fan, Structural mechanism of ligand activation in human calcium-sensing receptor, eLife, 5 (2016), https://doi.org/10.7554/eLife.13662.
[19] E.M. Brown, Role of the calcium-sensing receptor in extracellular calcium homeostasis, Best. Prac. Res. Clinic. Endo. Metabol. 27 (3) (2013) 333–343, https://doi.org/10.1016/j.beem.2013.02.006.
[20] C.E. Gibbons, D. Maldonado-Pérez, A.N. Shah, D. Riccardi, D.T. Ward, Calcium-sensing receptor antagonism or lithium treatment ameliorates aminoglycoside-induced cell death in renal epithelial cells, Biochim. Biophy. Acta. 1782 (2008) 188–195, https://doi.org/10.1016/j.bbadis.2008.01.003.
[21] S. Basith, M. Cui, S.J.Y. Macalino, J. Park, N.A.B. Clavio, S. Kang, S. Choi, Exploring G protein-coupled receptors (GPCRs) ligand space via cheminformatics approaches: imapct on rational drug design, Frontiers. Pharmacol. 9 (128) (2018), https://doi.org/10.3389/fphar.2018.00128.
[22] J. Zhao, Y. Cao, L. Zhang, Exploring the computational methods for protein-ligand binding site prediction, Comp. Struc. Biotech. 18 (2020) 417–426, https://doi.org/10.1016/j.csbj.2020.02.008.
[23] S. Vajda, F. Guarnieri, Characterization of protein-ligand interaction sites using experimental and computational methods, Curr. Opin. Drug. Discov. Develop 9 (354) (2006).
[24] T.A. Rants'o, C.J. van der Westhuizen, R.L. van Zyl, Optimization of covalent docking for organophosphates interaction with Anopheles acetylcholinesterase, J. Mol. Graph. Modell 110 (2022), https://doi.org/10.1016/j.jmgm.2021.108054.
[25] F.E. Boas, P.B. Harbury, Design of protein-ligand binding based on the molecular-mechanics energy model, J. Mol. Bio. 380 (2) (2008) 415–424, https://doi.org/10.1016/j.jmb.2008.04.001.
[26] F. Chen, H. Liu, H. Sun, P. Pan, Y. Li, D. Li, T. Hou, Assessing the performance of the MM/PBSA and MM/GBSA methods. 6. Capability to predict protein-protein binding free energies and re-rank binding poses generated by protein-protein docking, Physical.Chem.Chemical.Phys., 18(32) (2016), 22129–22139, https://doi.org/10.1039/c6cp03670h.
[27] T. Hou, J. Wang, Y. Li, W. Wang, Assessing the performance of the MM/PBSA and MM/GBSA methods. 1. The accuracy of binding free energy calculations based on molecular dynamics simulations, J.Chem.Info.Model., 51(1) (2011), 69–82, https://doi.org/10.1021/ci100275a.
[28] N. Homeyer, H. Gohlke, Free energy calculations by the molecular mechanics poisson−boltzmann surface area method, Mol. Inf. 31 (2012) 114–122, https://doi.org/10.1002/minf.201100135.
[29] G. Weng, E. Wang, F. Chen, H. Sun, Z. Wang, T. Hou, Assessing the performance of MM/PBSA and MM/GBSA methods. 9. Prediction reliability of binding affinities and binding poses for protein-peptide complexes, Physical.Chem.Chemical.Phys.,1 (19) (2019), 10135–10145, https://doi.org/10.1039/c9cp01674k.
[30] J. Li, R. Abel, K. Zhu, Y. Cao, S. Zhao, R.A. Friesner, The VSGB 2.0 model: a next generation energy model for high resolution protein structure modeling, Proteins 79 (2011) 2794–2812, https://doi.org/10.1002/prot.23106.
[31] H. Liu, P. Yi, W. Zhao, Y. Wu, F. Acher, J.P. Pin, J. Liu, P. Rondard, Illuminating the allosteric modulation of the calcium-sensing receptor, PNAS. 117 (2020) 21711–21722, https://doi.org/10.1073/pnas.1922231117.
[32] C. Lu, C. Wu, D. Ghoreishi, W. Chen, L. Wang, W. Damm, G.A. Ross, M.K. Dahlgren, E. Russell, C.D. Von Bargen, R. Abel, R.A. Friesner, E.D. Harder, *OPLS4*: improving force field accuracy on challenging regimes of chemical space, J. Chem. Theory. Comput. 17 (2021) 4291–4300, https://doi.org/10.1021/acs.jctc.1c00302.
[33] J. Diao, A. DeBono, T.M. Josephs, J.E. Bourke, B. Capuano, J. Karen, J. Gregory, K. Leach, Therapeutic opportunities of targeting allosteric binding sites on the calcium-sensing receptor, Acs.pharmacol. Transl. Sci. 4 (2021) 666–679, https://doi.org/10.1021/acsptsci.1c00046.
[34] J.A. Erickson, M. Jalaie, D.H. Robertson, R.A. Lewis, M. Vieth, Lessons in molecular recognition: the effects of ligand and protein flexibility on molecular docking accuracy, J. Med. Chem. 47 (1) (2004) 45–55, https://doi.org/10.1021/jm030209y.
[35] X. Chen, L. Wang, Q. Cui, Z. Ding, L. Hin, Y. Kou, W. Zhang, X. Jia, M. Dai, Z. Shi, Y. Li, Y. Geng, Structural insights into the activation of human calcium-sensing receptor, eLife, 10 (2021), https://doi.org/10.7554/eLife.68578.
[36] L. Tian, S. Liu, S. Wang, L. Wang, Ligand-binding specificity and promiscuity of main lignocellulolytic enzyme families as revealed by active-site architecture analysis, Sci. Rep 6 (2016), https://doi.org/10.1038/srep23605.
[37] D. Chen, N. Oezguen, P. Urvil, C. Ferguson, S.M. Dann, T.C. Savidge, Regulation of protein-ligand binding affinity by hydrogen bond pairing, Sci. Adv. 2 (3) (2016), https://doi.org/10.1126/sciadv.1501240.
[38] M.K. Haider, H.O. Bertrand, R.E. Hubbard, Predicting fragment binding poses using a combined MCSS MM-GBSA approach, J. Chem. Inf. Model. 51 (5) (2011) 1092–1105, https://doi.org/10.1021/ci100469n.

[39] B. Ma, M. Shatsky, H.J. Wolfson, R. Nussinov, Multiple diverse ligands binding at a single protein site: a matter of pre-existing populations, Prot. Sci. 11 (2) (2002) 184–197, https://doi.org/10.1110/ps.21302.
[40] H.X. Zhou, X. Pang, Electrostatic interactions in protein structure, folding, binding, and condensation, Chem. Rev. 118 (4) (2018) 1691–1741, https://doi.org/10.1021/acs.chemrev.7b00305.
[41] C. Chen, M.J. Hour, W.C. Lin, K. Wong, L. Shiao, K. Cheng, P. Chan, Y. Leung, Antagonism of Ca2+-sensing receptors by NPS 2143 is transiently masked by p38 activation in mouse brain bEND.3 endothelial cells, Naunyn-Schmiedeberg's, Arch. Pharmacol. 392 (2019) 823–832, https://doi.org/10.1007/s00210-019-01637-y.
[42] J.W. Lee, H.A. Park, O.K. Kwon, J.W. Park, G. Lee, H.J. Lee, S.J. Lee, S.R. Oh, K. S. Ahn, NPS 2143, a selective calcium-sensing receptor antagonist inhibits lipopolysaccharide-induced pulmonary inflammation, Mol. Immunol. 90 (2017) 150–157, https://doi.org/10.1016/j.molimm.2017.07.012.
[43] R. Reimschuessel, C.M. Gieseker, R.A. Miller, J.L. Ward, J.L. Boehmer, N.G. Rummel, D.N. Heller, C.B. Nochetto, G.K. de Alwis, N. Bataller, W.C. Andersen, S.B. Turnipseed, C.M. Karbiwnyk, R.D. Satzger, J.B. Crowe, N.Wilber, M.K. Reinhard, J. F. Roberts, M.R. Witkowski, Evaluation of the renal effects of experimental feeding of melamine and cyanuric acid to fish and pig, Amer.J.Vet.Res., 69 (9) (2008), 1217-1228, https://doi.org/10.2460/ajvr.69.9.1217.
[44] S. Taksinoros, H. Murata, Effects of serum proteins on in vitro melamine-cyanurate crystal formation, J. Vet. Med. Sci. 74 (12) (2012) 1569–1573, https://doi.org/10.1292/jvms.12-0138.
[45] J.W. Kaus, E. Harder, T. Lin, R. Abel, J.A. McCammon, L. Wang, How to deal with multiple binding poses in alchemical relative protein–ligand binding free energy calculations, J. Chem. Theor. Comput. 11 (6) (2015) 2670–2679, https://doi.org/10.1021/acs.jctc.5b00214.
[46] S. Genheden, U. Ryde, The MM/PBSA and MM/GBSA methods to estimate ligand binding affinities, Expet Opin. Drug Discov. 10 (5) (2015) 449–461, https://doi.org/10.1517/17460441.2015.1032936.
[47] F. Biederman, H.J. Schneider, Experimental binding energies in supramolecular complexes, Chem. Rev. 116 (2016) 5216–5300, https://doi.org/10.1021/acs.chemrev.5b00583.
[48] W. Sun, X. Chen, Y. Mei, X. Li, Y. Yang, L. An, Co-exposure of melamine and cyanuric acid as a risk factor for oxidative stress and energy metabolism: adverse effects on hippocampal neuronal and synaptic function induced by excessive ROS production, Ecotoxicol. Environ. Saf. 247 (2022), https://doi.org/10.1016/j.ecoenv.2022.114230.
[49] R.L. Dobson, S. Motlagh, M. Quijano, R.T. Cambron, T.R. Baker, A.M. Pullen, B. T. Regg, A.S. Bigalow-Kern, A. Vennard, A. Fix, R. Reimschuessel, G. Overmann, Y. Shan, G.P. Daston, Identification and characterization of toxicity of contaminants in pet food leading to an outbreak of renal toxicity in cats and dogs, J. Tox. Sci. 106 (1) (2008) 251–262, https://doi.org/10.1093/toxsci/kfn160.
[50] S.M. Cohen, Crystalluria and chronic kidney disease, Tox. Path. 48 (8) (2018) 949–955, https://doi.org/10.1177/0192623318800711.
[51] R.P. Dalal, D.S. Goldfarb, Melamine-related kidney stones and renal toxicity, Nat. Rev. Nephrol. 7 (2011) 267–274, https://doi.org/10.1038/nrneph.2011.24.
[52] J.L. Fisher, K.T. Williams, L.J. Schneider, A.J. Keebaugh, C.L. German, A.M. Hott, N. Singh, R.A. Clewell, Evaluation of QSAR models for tissue-specific predictive toxicology and risk assessment of military-relevant chemical exposures: a systematic review, Comput. Toxicol. 32 (2024), https://doi.org/10.1016/j.comtox.2024.100329.